**Supporting information**

# Electrochemical $H_2$ evolution promoted by a bioinspired (N2S2)Ni(II) complex

*Soumalya Sinha,[†,#] Giang N. Tran,[†,#] Hanah Na,[†] and Liviu M. Mirica[†,*]*

[†]Department of Chemistry, University of Illinois at Urbana-Champaign, Urbana, Illinois, 61801

[#] These authors contributed equally

*E-mail: mirica@illinois.edu

## Table of Contents

## 1. General experimental details

### Reagents and Materials

All reagents were commercially available from Sigma-Aldrich, Fisher Scientific or Strem Chemicals and were used as received without further purification. N2S2 was synthesized following a published procedure.[1, 2] Solvents were purified prior to use by passing through a column of activated alumina using an M Braun solvent purification system.

### Physical Measurements

$^1$H NMR spectra were recorded on a Bruker 500 spectrometer (500 MHz) at UIUC School of Chemical Sciences NMR Lab. Chemical shifts are reported in ppm and referenced to residual solvent resonance peaks. UV-vis spectra were recorded on a Varian Cary 50 Bio spectrophotometer and are reported as $\lambda_{max}$, nm ($\varepsilon$, $M^{-1}$ $cm^{-1}$). EPR spectra were recorded on a JEOL JES-FA X-band (9.2 GHz) or a Bruker 10" EMXPlus X-band Continuous Wave EPR spectrometer at 77 K. EPR spectra simulation and analysis were performed using Bruker WINEPR SimFonia program, version 1.25. Elemental analysis was carried out by the Microanalysis Laboratory at UIUC using an Exeter Analytical Model CE440 CHN Analyzer. ESI-MS experiments were performed by the Mass Spectrometry Lab at UIUC using a Waters Q-TOF Ultima ESI mass spectrometer with an electron spray ionization source.

### Electrochemistry

Electrochemical experiments were carried out using BASi Epsilon and CH Instruments potentiostats. Cyclic voltammetry used a conventional three-electrode cell with a glassy carbon (GC) working electrode (surface area = 0.07 $cm^2$), a non-aqueous Ag/0.01 M $AgNO_3$/MeCN reference electrode, and a Pt wire counter electrode. The GC electrode was prepared by polishing on a cloth polishing pad using 5-micron aluminum oxide polishing slurry, followed by a thorough deionized water rinse, and gently drying with a heat gun.[3] Cyclic voltammograms (CVs) were recorded by dissolving the metal complexes to 1.5 mM in 0.1 M of $^n$Bu$_4$NPF$_6$ (TBAP) in MeCN, with or without the addition of protic additives, at 0.1 V/s scan rate unless otherwise noted. Ferrocene was used as an external standard for all the

electrochemical experiments, and all potentials are reported with respect to the ferrocenium-ferrocene couple ($Fc^{+/0}$).[4] All CV data are plotted according to the US convention,[3] where the positive and negative currents are for the reduction and oxidation processes, respectively.

## 2. Preparation of $[(N2S2)Ni(MeCN)_2]^{2+}$ ($1^{2+}$)

**Method 1:**

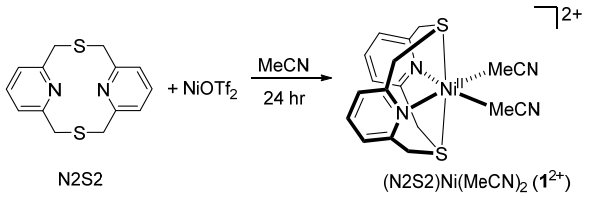


A suspension of $Ni(OTf)_2$ (66.32 mg, 0.185 mmol) in MeCN was added to a suspension of N2S2 in MeCN (51 mg, 0.185 mmol). The solution mixture was stirred at room temperature for 24 hours, after which a cloudy solution formed. The precipitate was separated by filtration, and the purple filtrate was collected. To the filtrate was added $Et_2O$ (10 mL) to crash out the product. The supernatant was removed, and the purple solid was dried under vacuum. X-ray quality crystals were obtained by slow $Et_2O$ diffusion into a MeCN solution at room temperature. Yield: 95.6 mg, 81.5%.

**Method 2:**

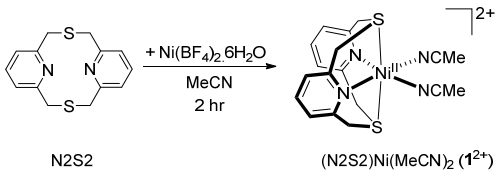


The complex was prepared under air. A solution of $Ni(BF_4)_2{\cdot}6H_2O$ (24.8 mg, 0.0728 mmol) in acetonitrile was added to a suspension of N2S2 (20 mg, 0.0728 mmol) in acetonitrile, and the reaction mixture turned light purple. After stirring for 2 hours, the solution was filtered and concentrated for recrystallization by diethyl ether diffusion. Purple crystals formed, and the supernatant was removed. The resulting solid was washed with $Et_2O$ and dried in *vacuo*. The product $[(N2S2)Ni(MeCN)_2](BF_4)_2$ was isolated as a purple solid. Yield: 33 mg, 77%.

**Method 3:**

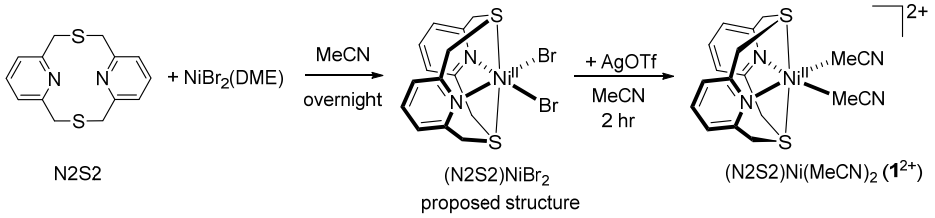


A solution of $NiBr_2$(DME) (18.8 mg, 0.061 mmol) in MeCN was added to a suspension of N2S2 (16.7 mg, 0.061 mmol) in MeCN. Green solid crashed out of the solution and the reaction mixture was stirred overnight. To the suspension of $N2S2NiBr_2$ in MeCN was added AgOTf (15.6 mg, 0.061 mmol) solution in MeCN. The color of the solution changed to light purple and very light-yellow solids precipitated. The solution mixture was run through a syringe filter to separate AgBr salt. A light purple solid precipitated out of the filtrate by adding an excess amount of $Et_2O$. The precipitate was then filtered and washed with $Et_2O$ (3 mL) and dried under vacuum. Yield: 38.9 mg, 89.6%.

Elemental analysis: found, C 36.00, H 3.40 N 8.86%; calculated $C_{18}H_{20}B_2F_8N_4NiS_2 \cdot H_2O$, C 35.63., H 3.65, N 9.23%.

UV-Vis (MeCN; λ nm (ε, $M^{-1}$ $cm^{-1}$)): 262 (200), 289 (67).

## 3. Electrochemical studies

### Cyclic voltammograms (CVs) for bare glassy carbon (GC) electrode

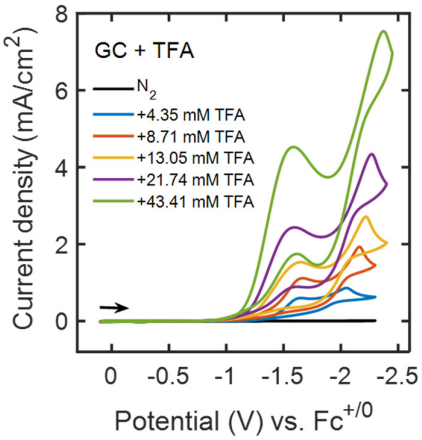


**Figure S1.** CVs recorded for bare GC electrode in $N_2$-saturated 0.1 M TBAP/MeCN solution in the absence (black) and the presence of different concentrations of TFA (4.35 mM - 43.41 mM) as shown in the legend. All CVs were recorded at 0.1 V/s scan rate. The arrow shown in the figure indicates the direction of the CV recorded.

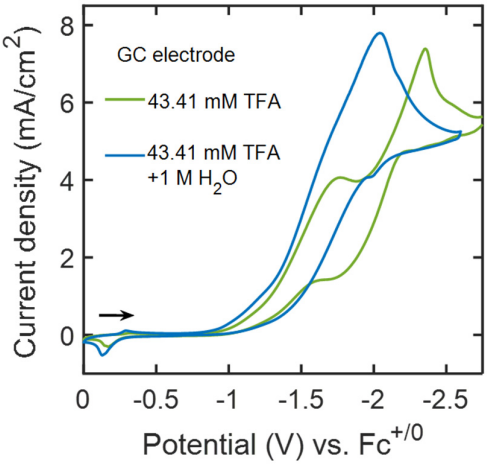


**Figure S2.** CVs recorded for bare GC electrode in $N_2$-saturated 0.1 M TBAP/MeCN solution in the presence of 43.41 mM of TFA (green) and 43.41 mM TFA + 1 M $H_2O$ (blue). All CVs were recorded at 0.1 V/s scan rate. The arrow shown in the figure indicates the direction of the CV recorded.

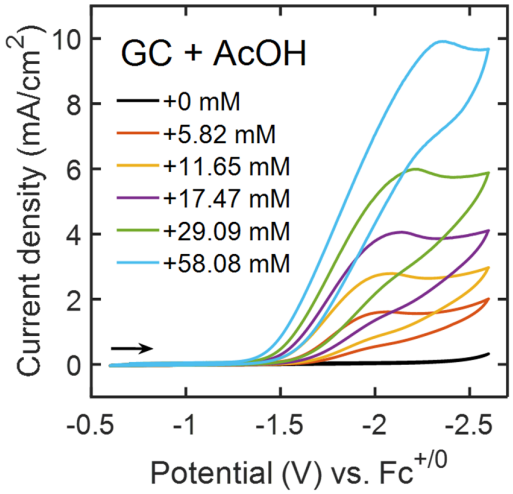


**Figure S3.** CVs recorded for bare GC electrode in $N_2$-saturated 0.1 M TBAP/MeCN solution in the absence (black) and the presence of different concentrations of AcOH (5.82 mM – 58.08 mM) as shown in the legend. All CVs were recorded at 0.1 V/s scan rate. The arrow shown in the figure indicates the direction of the CV recorded.

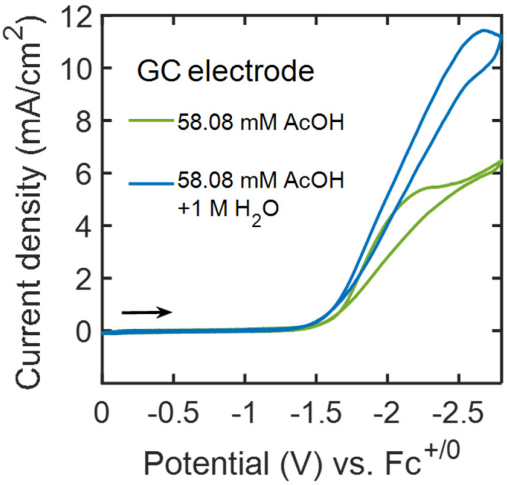


**Figure S4.** CVs recorded for bare GC electrode in $N_2$-saturated 0.1 M TBAP/MeCN solution in the presence of 58.08 mM of AcOH (green) and 58.08 mM AcOH + 1 M $H_2O$ (blue). All CVs were recorded at 0.1 V/s scan rate. The arrow shown in the figure indicates the direction of the CV recorded.

**Cyclic voltammograms (CVs) for $[(N2S2)Ni(MeCN)_2]^{2+}$ ($\mathbf{1}^{2+}$)**

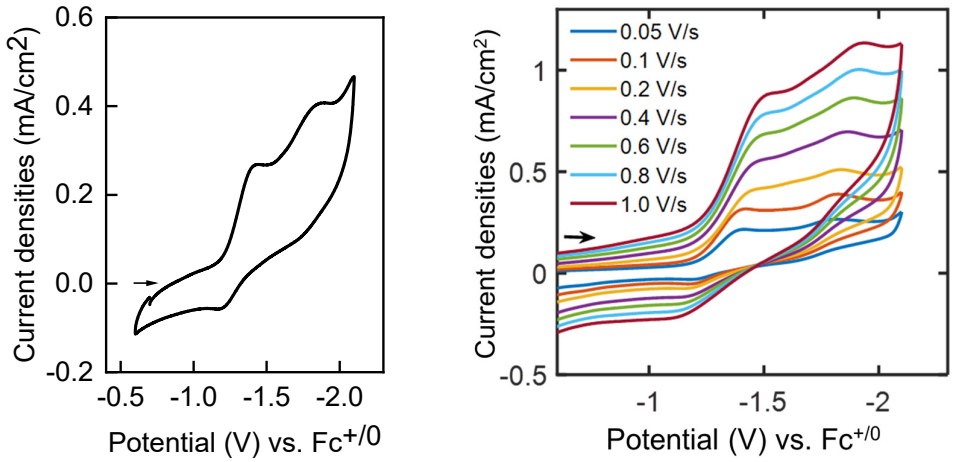


**Figure S5.** a) CV of $\mathbf{1}^{2+}$ in $N_2$-saturated 0.1 M TBAP/MeCN solution. Scan rate = 0.1 V/s; b) CVs recorded for $\mathbf{1}^{2+}$ in $N_2$-saturated 0.1 M TBAP/MeCN solution at different scan rates (0.1 V/s – 1.0 V/s). The arrow shown in the figure indicates the direction of the scan.

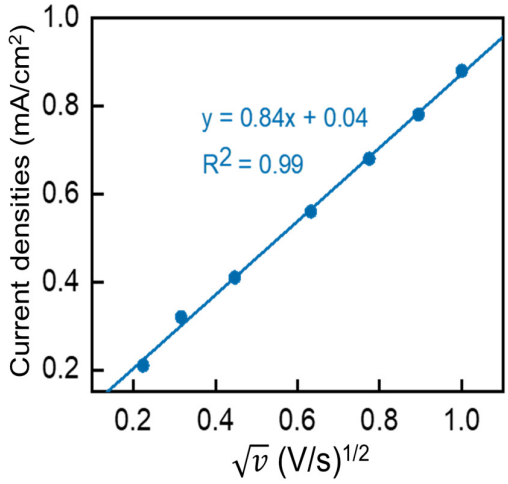


**Figure S6.** Peak current densities obtained at the $Ni^{II/I}$ reduction wave for $\mathbf{1}^{2+}$ in $N_2$-saturated 0.1 M TBAP/MeCN solution at different scan rates (0.1 V/s – 1.0 V/s) are plotted versus square root of the scan rates.

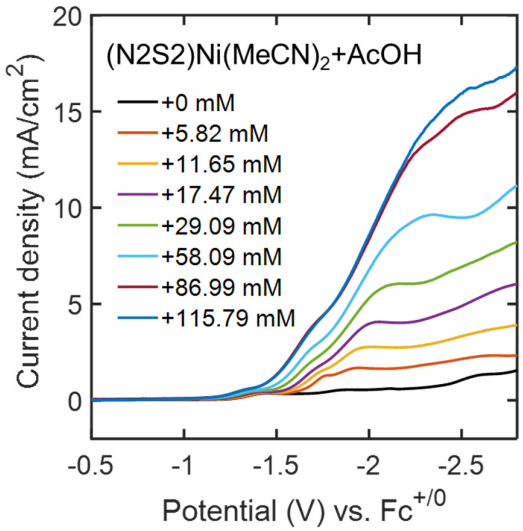


**Figure S7.** CVs recorded for $\mathbf{1}^{2+}$ in $N_2$-saturated 0.1 M TBAP/MeCN solution in the absence (black) and the presence of different concentrations of AcOH (5.82 mM – 115.79 mM) as shown in the legend. All CVs were recorded at 0.1 V/s scan rate. Only forward reductive scans are shown for clarity.

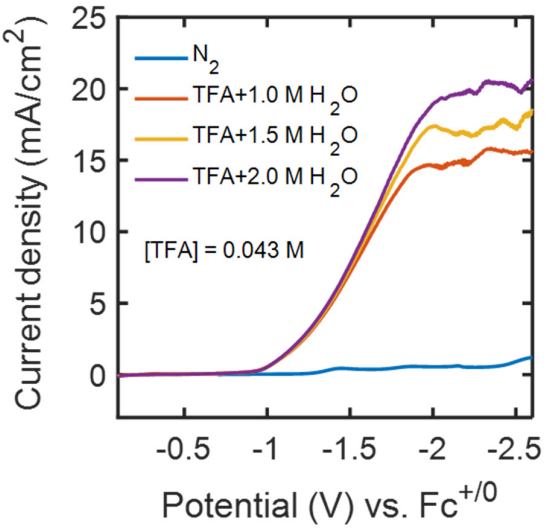


**Figure S8.** Linear sweep voltammograms for $\mathbf{1}^{2+}$ recorded in $N_2$-saturated 0.1 M TBAP/MeCN in the absence of TFA (blue) and in the presence of 0.043 M TFA + different concentration of $H_2O$, 1 M (orange), 1.5 M (yellow), and 2.0 M (purple). Scan rate = 0.1 V/s. The uneven features at the plateau-current regions could be due to the formation of $H_2$ bubbles at the surface of the electrode.

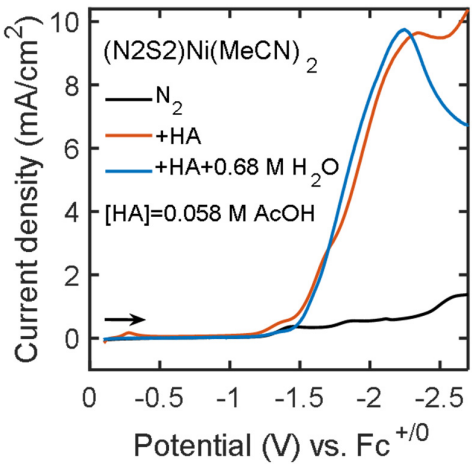


**Figure S9.** CVs recorded for $\mathbf{1}^{2+}$ in $N_2$-saturated 0.1 M TBAP/MeCN in the absence of AcOH (black), in the presence of 0.058 M AcOH (orange), and 0.058 M AcOH + 0.68 M $H_2O$ (blue). Only forward scans are shown for clarity. Scan rate = 0.1 V/s.

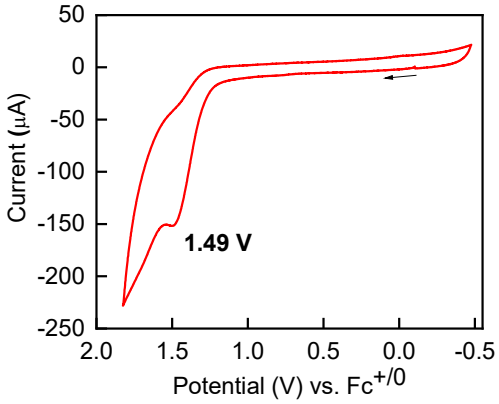


**Figure S10.** CVs recorded for $\mathbf{1}^{2+}$ in $N_2$-saturated 0.1 M TBAP/MeCN within the electrochemical window between –0.5 V and 2.0 V vs. $Fc^{+/0}$. Scan rate = 0.1 V/s.

**Comparative cyclic voltammograms (CVs)**

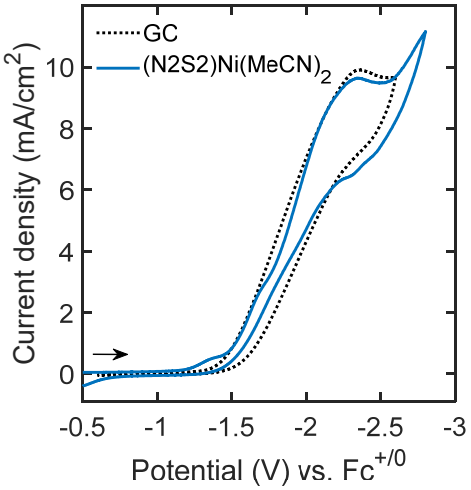


**Figure S11.** Comparative CVs collected for bare glassy carbon (black dotted line) and $\mathbf{1}^{2+}$ (blue solid line) in $N_2$-saturated 0.1 M TBAP/MeCN + 0.058 M AcOH.

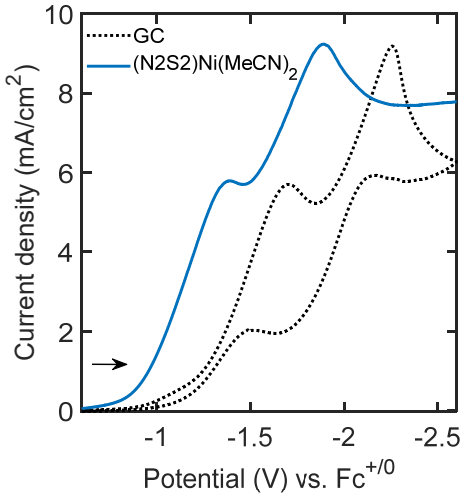


**Figure S12.** Comparative CVs collected for bare glassy carbon (black dotted line) and $\mathbf{1}^{2+}$ (blue solid line) in $N_2$-saturated 0.1 M TBAP/MeCN + 0.043 M TFA. Only reductive waves for $\mathbf{1}^{2+}$ is shown for clarity.

**Chronoamperometric measurements**

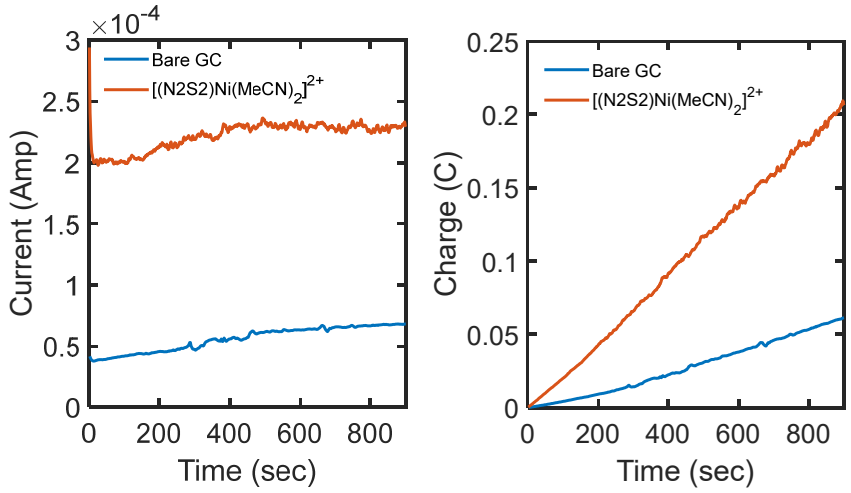


**Figure S13.** Left: Chronoamperometric experiments performed for bare glassy carbon electrode (blue) and $\mathbf{1}^{2+}$ (orange) in the presence of 0.043 M TFA and 1.5 M of $H_2O$ added in the TBAP/MeCN at the constant applied potential of $E_{cat/2}$. Right: The corresponding charges passed during the CPE experiments, as shown in the left.

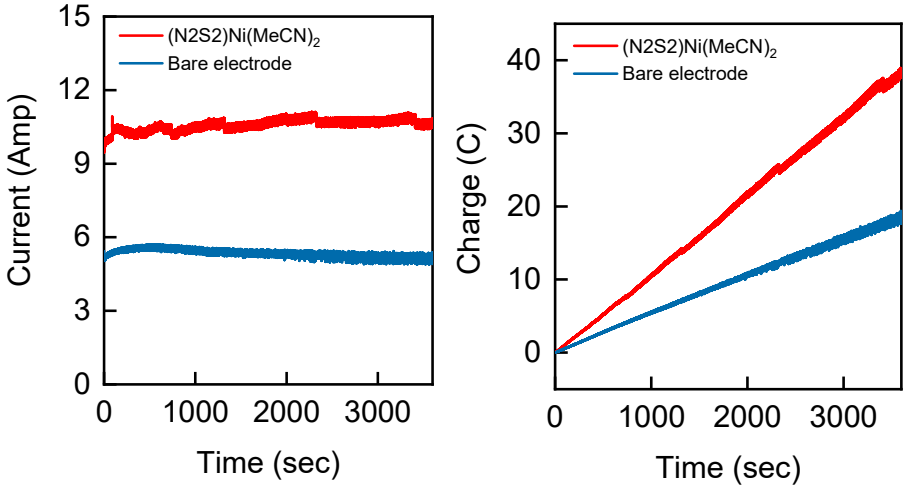


**Figure S14.** Left: Bulk electrolysis performed for bare carbon cloth electrode (blue, surface area = 1.5 $cm^2$) and $\mathbf{1}^{2+}$ (red) in the presence of 0.043 M TFA and 1.5 M of $H_2O$ added in the MeCN electrolyte at the constant applied potential of $E_{cat/2}$. Right: The corresponding charges passed during the CPE experiments, as shown in the left.

## 4. Gas chromatography data

Gas chromatography analysis was performed using Agilent Technologies 7890B GC system equipped with a thermal conductivity detector (TCD). Gas analytes were detected by passing through a HP-Molesieve column (30 m in length, 0.32 mm in diameter, and 25 µm film). The temperature for the detector was set at 220°C and 35°C for the oven. Helium was used as the carrier gas with a flow at 15 mL/min. The calibration curve for $H_2$ was determined by injecting the known quantities of pure $H_2$ in MeCN (same volume as used for the bulk electrolysis) in the electrolysis cell and by transferring the headspace. The gas sample from the headspace of the post-electrolysis cell was injected using an air-tight syringe (1 mL) and $H_2$ was detected as the negative peak area at the retention time of 1.72 min.

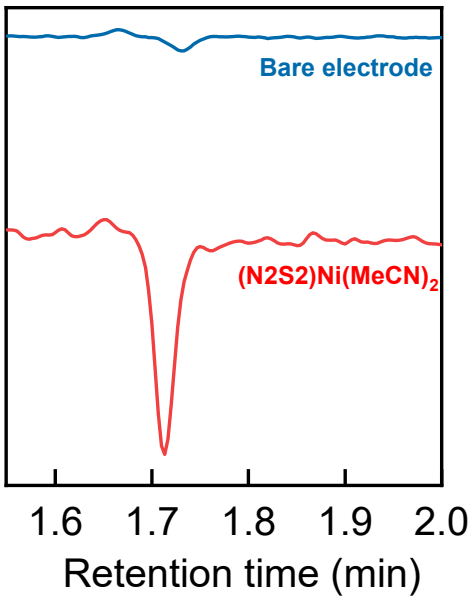


**Figure S15.** GC traces of $H_2$ observed for the bare carbon cloth electrode (blue) and $\mathbf{1}^{2+}$ (red) by transferring the headspace of the electrochemical cell after performing bulk electrolysis experiments in the presence of 0.043 M TFA + 1.5 M $H_2O$ in the MeCN electrolyte.

**5. Foot-of-the-wave analysis (FOWA)**

Foot-of-the-wave analysis on the CVs were performed by considering the ratio of catalytic current after subtracting the background currents due to the acid-only reduction, $i_c$ and peak current $i_p$. The equations for the catalytic current, $i_c$ and peak current, $i_p$ of an EECC mechanism can be written as,[5, 6]

$i_c = \frac{n_{cat}FAC_{cat}\sqrt{k_{FOWA}D_{cat}}}{[1+\exp(f(E-E_{1/2}))]}$; Eq. S1

$i_p = 0.4463\, nFAC_{cat}\sqrt{nfvD_{cat}}$; Eq. S2

where,

$n_{cat}$ = required number of electrons in catalysis = 2 (for hydrogen evolution)

F = Faraday constant = 96485 C/mol

A = electrode surface area

$C_{cat}$ = concentration of the catalysts

$k_{FOWA}$ = pseudo-first-order reaction rate constant in $sec^{-1}$

$D_{cat}$ = diffusion coefficient of the catalyst

$f$ = F/RT = 38.94 $V^{-1}$

$E$ = applied potential obtained from the CV

$E_{1/2}$ = Potential at $Ni^{II/I}$ reduction

$n$ = number of noncatalytic electrons = 1

$v$ = scan rate

Dividing Eq. S1 by Eq. S2 and inserting the numerical values for as given above, we can obtain the Eq. S3 for the FOWA,

$\frac{i_c}{i_p} = \frac{0.7179\sqrt{\frac{k_{FOWA}}{v}}}{[1+\exp(f(E-E_{cat}))]}$; Eq. S3

In our work, we measured $i_p$ as the height of the peak current obtained at the $Ni^{II/I}$ redox wave for both the catalysts and scan rate was 0.1 V/s.

**FOWA for $[(N2S2)Ni(MeCN)_2]^{2+}$ ($1^{2+}$)**

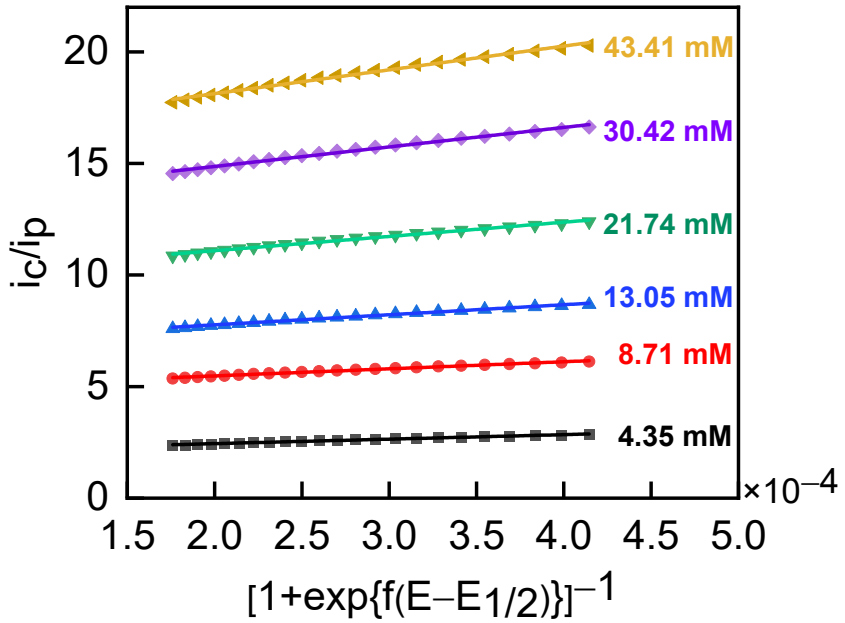


**Figure S16.** FOWA for $\mathbf{1}^{2+}$ in $N_2$-saturated 0.1 M $TBAPF_6$/MeCN in the presence of different concentration of TFA (4.35 mM – 43.41 mM). The most linear portion at the lower range of 1/1+exp(f(E-$E_{1/2}$)) values that corresponds to the applied potentials near to the onset potentials between –0.9 V and –1.1 V were fitted linearly. $R^2$ values for all the linear fits are greater than 0.97.

**Table S1.** Rate constants for the first chemical step estimated for $[(N2S2)Ni(MeCN)_2]^{2+}$ in $N_2$-saturated MeCN electrolyte in the presence of different TFA concentrations.

| Concentration of TFA (mM) | Slope obtained from the FOWA | $k_{FOWA}$ ($sec^{-1}$) |
|---|---|---|
| 4.35 | 3798.63 | $2.78\times10^6$ |
| 8.71 | 5849.41 | $6.6\times10^6$ |
| 13.05 | 8446.98 | $1.38\times10^7$ |
| 21.74 | 11907.87 | $2.74\times10^7$ |
| 30.42 | 16273.39 | $5.11\times10^7$ |
| 43.41 | 20010.60 | $7.72\times10^7$ |

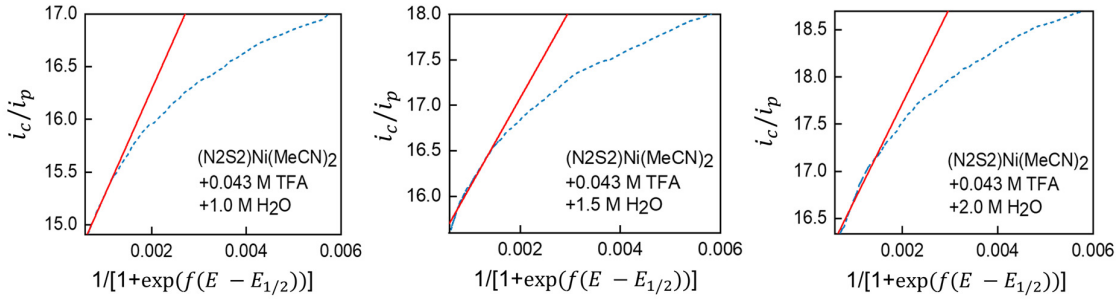


**Figure S17.** FOWA for $\mathbf{1}^{2+}$ in $N_2$-saturated 0.1 M $TBAPF_6$/MeCN + 0.043 M of TFA at different concentration of $H_2O$; 1 M (left), 1.5 M (middle), and 2.0 M (right). The most linear portion at the lower range of 1/1+exp(f(E-$E_{1/2}$)) values are fitted linearly. $R^2$ values for all the linear fits are greater than 0.97.

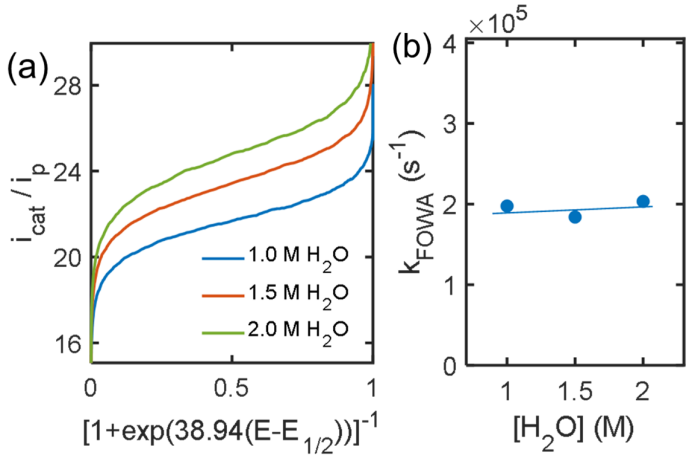


**Figure S18.** (a) FOWA for $\mathbf{1}^{2+}$ in $N_2$-saturated 0.1 M TBAP/MeCN + 0.043 M TFA at different concentration of $H_2O$; 1 M (blue), 1.5 M (orange), and 2 M (yellow). The most linear portion at the lower range of 1/1+exp(38.94(E-$E_{1/2}$)) values are fitted linearly to extract the rate constant ($k_{FOWA}$, $s^{-1}$). (b) The $k_{FOWA}$ values obtained from (a) are plotted vs. the concentration of $H_2O$.

**Table S2.** Rate constants estimated for $[(N2S2)Ni(MeCN)_2]^{2+}$ in $N_2$-saturated MeCN electrolyte + 0.043 M TFA at different $H_2O$ concentrations.

| Concentration of $H_2O$ | Slope obtained from the FOWA | $k_{FOWA}$ ($sec^{-1}$) | Average $k_{FOWA}$ ($sec^{-1}$) |
|---|---|---|---|
| 1.0 M | 1009.15 | $1.98\times10^5$ | $(1.95\pm0.01)\times10^5$ |
| 1.5 M | 973.62 | $1.84\times10^5$ | |
| 2.0 M | 1023.74 | $2.03\times10^5$ | |

## 6. UV-vis Absorption spectra

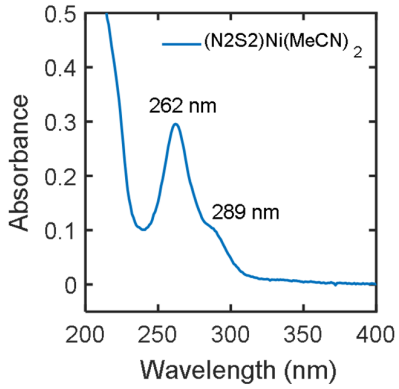


**Figure S19.** Absorption spectrum collected for $\mathbf{1}^{2+}$ (1.5 mM) in MeCN solution.

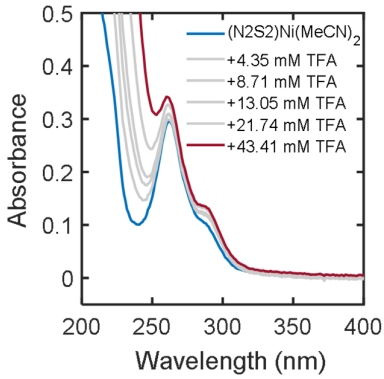


**Figure S20.** Absorption spectra collected for $\mathbf{1}^{2+}$ (1.5 mM) in the MeCN solution in the absence of TFA (blue) and in the presence of a different concentration of TFA (4.35 mM – 43.41 mM) as shown in the legend.

## 7. EPR studies of Ni complexes

*General procedure EPR analysis.* An EPR tube was charged with a solution of Ni complex in 1:3 MeCN:PrCN (butyronitrile), which was cooled in an acetone/dry ice cold bath. To that solution was added a 1:3 MeCN:PrCN solution containing 1 equiv of $CoCp^*_2$. The resulting solution was shaken for 5 seconds and then frozen in liquid nitrogen. Typical experimental conditions: frequency ≈ 9.096 GHz, power = 1 mW, modulation frequency = 100 kHz, modulation amplitude = 3 G, time constant = 0.3 s, linewidth = 15 G.

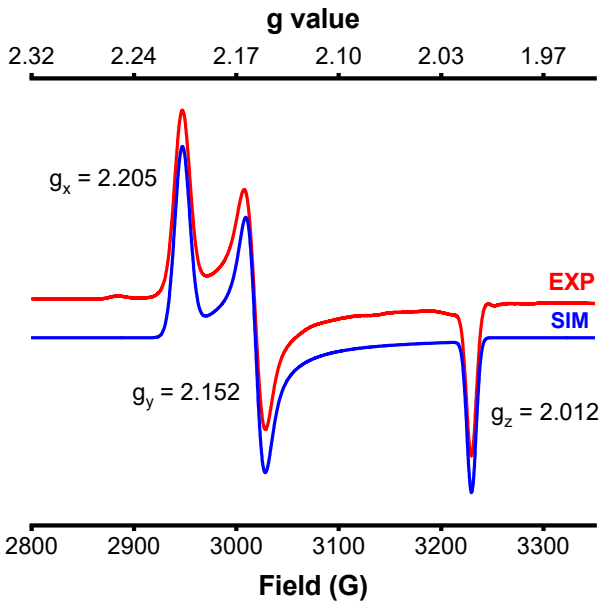


**Figure S21.** EPR spectrum of $\mathbf{1}^{2+}$ + $CoCp^*_2$ in 1:3 MeCN:PrCN glass, 77K.

## 8. X-ray crystal structure characterization

*General information:* Suitable crystals of appropriate dimensions were mounted on Mitgen loops in random orientations. Preliminary examination and data collection were performed using a Bruker Kappa Apex-II Charge Coupled Device (CCD) Detector system single crystal X-ray diffractometer equipped with an Oxford Cryosteam LT device. Data were collected using graphite monochromated MO Kα radiation (λ = 0.71073 Å) from a fine focus sealed tube X-ray source. Preliminary unit cell constants were determined with a set of 36 narrow frame scans. Typical data sets consist of a combination of ϖ and φ scan frames with typical scan width of 0.5º and counting time of 15-30 seconds/frame at a crystal to detector distance of ~4.0 cm. The collected frames were integrated using an orientation matrix determined from the narrow frame scans. Apex II and SAINT software packages (*Bruker Analytical X-Ray, Madison, WI, 2008*) were used for data collection and data integration. Analysis of the integrated data did not show any decay. Final cell constants were determined by global refinement of reflections from the complete data set. Data were corrected for systematic errors using SADABS (*Bruker Analytical X-Ray, Madison, WI, 2008*) based on the Laue symmetry using equivalent reflections. Structure solutions and refinement were carried out using the SHELXTL- PLUS software package.[7] The structures were refined with full matrix least-squares refinement by minimizing $\Sigma w(Fo^2-Fc^2)^2$. All non-hydrogen atoms were refined anisotropically to convergence. Typically, H atoms are added at the calculated positions in the final refinement cycles. The structure of $[(N2S2)Ni(MeCN)_2](OTf)_2$ was deposited into the Cambridge Structural Database, deposition number CCDC 2053835.

**X-ray structure determination of $[(N2S2)Ni(MeCN)_2](OTf)_2$ ($1•(OTf)_2$, CCDC 2053835)**

**Table S3.** Crystal data and structure refinement for **$1•(OTf)_2$**

| | | |
|---|---|---|
| Identification code | l10316/lt/X8/GT32-N2S2NiOTf2 | |
| Empirical formula | $C_{20}$ $H_{20}$ $F_6$ $N_4$ Ni $O_6$ $S_4$ | |
| Formula weight | 713.35 | |
| Temperature | 100(2) K | |
| Wavelength | 0.71073 Å | |
| Crystal system | Monoclinic | |
| Space group | $P2_1/n$ | |
| Unit cell dimensions | a = 11.1552(4) Å | α= 90°. |
| | b = 22.3576(7) Å | β= 112.8623(15)°. |
| | c = 11.9838(4) Å | γ = 90°. |
| Volume | 2754.00(16) $Å^3$ | |
| Z | 4 | |
| Density (calculated) | 1.720 $Mg/m^3$ | |
| Absorption coefficient | 1.093 $mm^{-1}$ | |
| F(000) | 1448 | |
| Crystal size | 0.297 x 0.253 x 0.235 $mm^3$ | |
| Theta range for data collection | 1.822 to 40.328°. | |
| Index ranges | -19≤h≤20, -40≤k≤40, -21≤l≤21 | |
| Reflections collected | 74511 | |
| Independent reflections | 17300 [R(int) = 0.0527] | |
| Completeness to theta = 25.242° | 99.9 % | |
| Absorption correction | Semi-empirical from equivalents | |
| Max. and min. transmission | 0.8028 and 0.7354 | |
| Refinement method | Full-matrix least-squares on $F^2$ | |
| Data / restraints / parameters | 17300 / 0 / 372 | |
| Goodness-of-fit on $F^2$ | 1.021 | |
| Final R indices [I>2sigma(I)] | R1 = 0.0383, wR2 = 0.0791 | |
| R indices (all data) | R1 = 0.0675, wR2 = 0.0896 | |
| Largest diff. peak and hole | 0.748 and -0.435 $e.Å^{-3}$ | |

**Table S4.** Bond lengths [Å] and angles [°] for **1•(OTf)$_2$**

| | |
|---|---|
| Ni(1)-N(4) | 2.0392(10) |
| Ni(1)-N(2) | 2.0590(9) |
| Ni(1)-N(3) | 2.0602(10) |
| Ni(1)-N(1) | 2.0707(9) |
| Ni(1)-S(1) | 2.3796(3) |
| Ni(1)-S(2) | 2.3940(3) |
| S(1)-C(7) | 1.8060(12) |
| S(1)-C(6) | 1.8091(12) |
| S(2)-C(14) | 1.8094(11) |
| S(2)-C(13) | 1.8118(11) |
| N(1)-C(1) | 1.3467(14) |
| N(1)-C(5) | 1.3469(14) |
| N(2)-C(8) | 1.3434(14) |
| N(2)-C(12) | 1.3455(14) |
| N(3)-C(15) | 1.1428(14) |
| N(4)-C(17) | 1.1360(15) |
| C(1)-C(2) | 1.3894(15) |
| C(1)-C(14) | 1.5087(15) |
| C(2)-C(3) | 1.3830(17) |
| C(2)-H(2) | 0.9500 |
| C(3)-C(4) | 1.3860(17) |
| C(3)-H(3) | 0.9500 |
| C(4)-C(5) | 1.3905(15) |
| C(4)-H(4) | 0.9500 |
| C(5)-C(6) | 1.5069(16) |
| C(6)-H(6A) | 0.9900 |
| C(6)-H(6B) | 0.9900 |
| C(7)-C(8) | 1.4992(16) |
| C(7)-H(7A) | 0.9900 |
| C(7)-H(7B) | 0.9900 |
| C(8)-C(9) | 1.3900(15) |
| C(9)-C(10) | 1.3851(18) |
| C(9)-H(9) | 0.9500 |
| C(10)-C(11) | 1.3842(18) |
| C(10)-H(10) | 0.9500 |
| C(11)-C(12) | 1.3868(15) |

| | |
|---|---|
| C(11)-H(11) | 0.9500 |
| C(12)-C(13) | 1.5031(15) |
| C(13)-H(13A) | 0.9900 |
| C(13)-H(13B) | 0.9900 |
| C(14)-H(14A) | 0.9900 |
| C(14)-H(14B) | 0.9900 |
| C(15)-C(16) | 1.4514(15) |
| C(16)-H(16A) | 0.9800 |
| C(16)-H(16B) | 0.9800 |
| C(16)-H(16C) | 0.9800 |
| C(17)-C(18) | 1.4530(18) |
| C(18)-H(18A) | 0.9800 |
| C(18)-H(18B) | 0.9800 |
| C(18)-H(18C) | 0.9800 |
| S(4)-O(6) | 1.4400(10) |
| S(4)-O(4) | 1.4405(9) |
| S(4)-O(5) | 1.4422(9) |
| S(4)-C(20) | 1.8289(13) |
| F(4)-C(20) | 1.3354(16) |
| F(5)-C(20) | 1.3315(17) |
| F(6)-C(20) | 1.3302(16) |
| S(3)-O(1) | 1.4368(10) |
| S(3)-O(2) | 1.4398(9) |
| S(3)-O(3) | 1.4459(9) |
| S(3)-C(19) | 1.8244(13) |
| F(1)-C(19) | 1.3382(17) |
| F(2)-C(19) | 1.3369(15) |
| F(3)-C(19) | 1.3291(16) |

| | |
|---|---|
| N(4)-Ni(1)-N(2) | 91.46(4) |
| N(4)-Ni(1)-N(3) | 91.23(4) |
| N(2)-Ni(1)-N(3) | 175.96(4) |
| N(4)-Ni(1)-N(1) | 176.03(4) |
| N(2)-Ni(1)-N(1) | 85.39(3) |
| N(3)-Ni(1)-N(1) | 92.04(4) |
| N(4)-Ni(1)-S(1) | 96.61(3) |
| N(2)-Ni(1)-S(1) | 84.97(3) |
| N(3)-Ni(1)-S(1) | 91.72(3) |

| | |
|---|---|
| N(1)-Ni(1)-S(1) | 85.54(3) |
| N(4)-Ni(1)-S(2) | 92.65(3) |
| N(2)-Ni(1)-S(2) | 85.27(3) |
| N(3)-Ni(1)-S(2) | 97.61(3) |
| N(1)-Ni(1)-S(2) | 84.69(3) |
| S(1)-Ni(1)-S(2) | 166.703(11) |
| C(7)-S(1)-C(6) | 103.35(6) |
| C(7)-S(1)-Ni(1) | 96.84(4) |
| C(6)-S(1)-Ni(1) | 96.26(4) |
| C(14)-S(2)-C(13) | 102.67(5) |
| C(14)-S(2)-Ni(1) | 98.02(4) |
| C(13)-S(2)-Ni(1) | 94.11(4) |
| C(1)-N(1)-C(5) | 119.40(9) |
| C(1)-N(1)-Ni(1) | 120.91(7) |
| C(5)-N(1)-Ni(1) | 119.45(7) |
| C(8)-N(2)-C(12) | 119.83(9) |
| C(8)-N(2)-Ni(1) | 119.91(7) |
| C(12)-N(2)-Ni(1) | 119.00(7) |
| C(15)-N(3)-Ni(1) | 175.34(10) |
| C(17)-N(4)-Ni(1) | 169.69(10) |
| N(1)-C(1)-C(2) | 121.45(10) |
| N(1)-C(1)-C(14) | 119.64(9) |
| C(2)-C(1)-C(14) | 118.88(10) |
| C(3)-C(2)-C(1) | 119.20(10) |
| C(3)-C(2)-H(2) | 120.4 |
| C(1)-C(2)-H(2) | 120.4 |
| C(2)-C(3)-C(4) | 119.38(10) |
| C(2)-C(3)-H(3) | 120.3 |
| C(4)-C(3)-H(3) | 120.3 |
| C(3)-C(4)-C(5) | 118.73(11) |
| C(3)-C(4)-H(4) | 120.6 |
| C(5)-C(4)-H(4) | 120.6 |
| N(1)-C(5)-C(4) | 121.79(10) |
| N(1)-C(5)-C(6) | 119.26(9) |
| C(4)-C(5)-C(6) | 118.93(10) |
| C(5)-C(6)-S(1) | 116.36(8) |
| C(5)-C(6)-H(6A) | 108.2 |
| S(1)-C(6)-H(6A) | 108.2 |

| | |
|---|---|
| C(5)-C(6)-H(6B) | 108.2 |
| S(1)-C(6)-H(6B) | 108.2 |
| H(6A)-C(6)-H(6B) | 107.4 |
| C(8)-C(7)-S(1) | 115.45(8) |
| C(8)-C(7)-H(7A) | 108.4 |
| S(1)-C(7)-H(7A) | 108.4 |
| C(8)-C(7)-H(7B) | 108.4 |
| S(1)-C(7)-H(7B) | 108.4 |
| H(7A)-C(7)-H(7B) | 107.5 |
| N(2)-C(8)-C(9) | 121.49(10) |
| N(2)-C(8)-C(7) | 118.01(9) |
| C(9)-C(8)-C(7) | 120.42(10) |
| C(10)-C(9)-C(8) | 118.56(11) |
| C(10)-C(9)-H(9) | 120.7 |
| C(8)-C(9)-H(9) | 120.7 |
| C(11)-C(10)-C(9) | 119.80(11) |
| C(11)-C(10)-H(10) | 120.1 |
| C(9)-C(10)-H(10) | 120.1 |
| C(10)-C(11)-C(12) | 118.74(11) |
| C(10)-C(11)-H(11) | 120.6 |
| C(12)-C(11)-H(11) | 120.6 |
| N(2)-C(12)-C(11) | 121.45(10) |
| N(2)-C(12)-C(13) | 117.08(9) |
| C(11)-C(12)-C(13) | 121.42(10) |
| C(12)-C(13)-S(2) | 114.33(8) |
| C(12)-C(13)-H(13A) | 108.7 |
| S(2)-C(13)-H(13A) | 108.7 |
| C(12)-C(13)-H(13B) | 108.7 |
| S(2)-C(13)-H(13B) | 108.7 |
| H(13A)-C(13)-H(13B) | 107.6 |
| C(1)-C(14)-S(2) | 116.33(8) |
| C(1)-C(14)-H(14A) | 108.2 |
| S(2)-C(14)-H(14A) | 108.2 |
| C(1)-C(14)-H(14B) | 108.2 |
| S(2)-C(14)-H(14B) | 108.2 |
| H(14A)-C(14)-H(14B) | 107.4 |
| N(3)-C(15)-C(16) | 179.54(14) |
| C(15)-C(16)-H(16A) | 109.5 |

| | |
|---|---|
| C(15)-C(16)-H(16B) | 109.5 |
| H(16A)-C(16)-H(16B) | 109.5 |
| C(15)-C(16)-H(16C) | 109.5 |
| H(16A)-C(16)-H(16C) | 109.5 |
| H(16B)-C(16)-H(16C) | 109.5 |
| N(4)-C(17)-C(18) | 179.78(17) |
| C(17)-C(18)-H(18A) | 109.5 |
| C(17)-C(18)-H(18B) | 109.5 |
| H(18A)-C(18)-H(18B) | 109.5 |
| C(17)-C(18)-H(18C) | 109.5 |
| H(18A)-C(18)-H(18C) | 109.5 |
| H(18B)-C(18)-H(18C) | 109.5 |
| O(6)-S(4)-O(4) | 115.15(6) |
| O(6)-S(4)-O(5) | 114.75(6) |
| O(4)-S(4)-O(5) | 115.07(6) |
| O(6)-S(4)-C(20) | 103.31(6) |
| O(4)-S(4)-C(20) | 102.86(6) |
| O(5)-S(4)-C(20) | 103.27(6) |
| F(6)-C(20)-F(5) | 107.78(12) |
| F(6)-C(20)-F(4) | 107.18(11) |
| F(5)-C(20)-F(4) | 107.07(11) |
| F(6)-C(20)-S(4) | 111.28(9) |
| F(5)-C(20)-S(4) | 111.83(9) |
| F(4)-C(20)-S(4) | 111.46(10) |
| O(1)-S(3)-O(2) | 115.99(6) |
| O(1)-S(3)-O(3) | 114.82(6) |
| O(2)-S(3)-O(3) | 114.43(6) |
| O(1)-S(3)-C(19) | 103.49(6) |
| O(2)-S(3)-C(19) | 102.70(6) |
| O(3)-S(3)-C(19) | 102.86(6) |
| F(3)-C(19)-F(2) | 107.21(12) |
| F(3)-C(19)-F(1) | 107.79(11) |
| F(2)-C(19)-F(1) | 107.35(11) |
| F(3)-C(19)-S(3) | 111.13(9) |
| F(2)-C(19)-S(3) | 111.45(9) |
| F(1)-C(19)-S(3) | 111.69(10) |

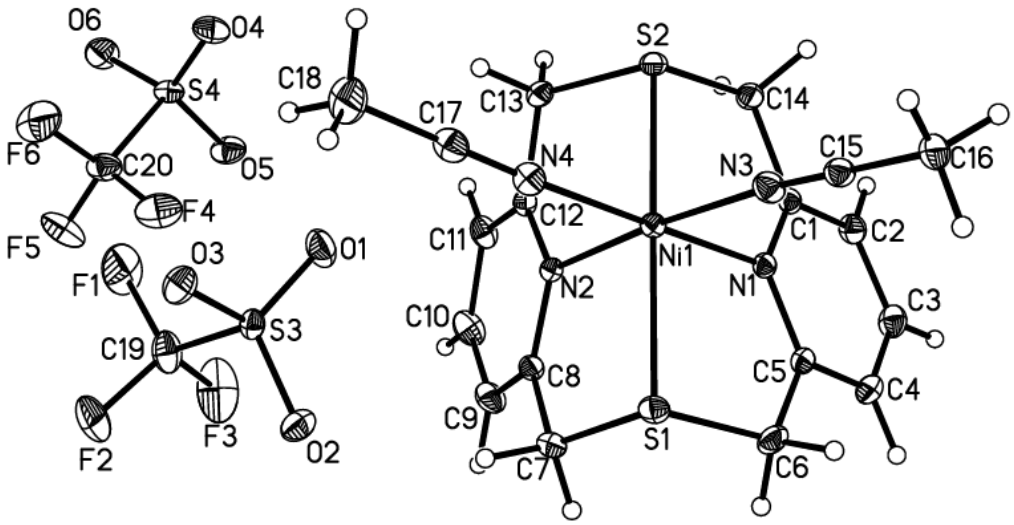


**Figure S22.** Projection view of **1•(OTf)$_2$** with 50% probability ellipsoids.

## 9. References


1. T. Moriguchi, S. Kitamura, K. Sakata and A. Tsuge, *Polyhedron*, 2001, **20**, 2315-2320.
2. C. Steeneck, O. Kinzel, C. Gege, G. Kleymann and T. Hoffmann, 2012.
3. N. Elgrishi, K. J. Rountree, B. D. McCarthy, E. S. Rountree, T. T. Eisenhart and J. L. Dempsey, *J. Chem. Educ.*, 2018, **95**, 197-206.
4. V. V. Pavlishchuk and A. W. Addison, *Inorg. Chim. Acta*, 2000, **298**, 97-102.
5. C. Costentin and J.-M. Savéant, *ChemElectroChem*, 2014, **1**, 1226-1236.
6. E. S. Rountree and J. L. Dempsey, *J. Am. Chem. Soc.*, 2015, **137**, 13371-13380.
7. G. M. Sheldrick, *Acta Cryst.*, 2008, **A64**, 112-122.